PCCP

Physical Chemistry Chemical Physics

www.rsc.org/pccp

Volume 12 | Number 39 | 21 October 2010 | Pages 12329–12876

ISSN 1463-9076

COVER ARTICLE
Chen *et al.*
NC unit trapped by fullerenes: a density functional theory study on $Sc_3NC@C_{2n}$ (2*n*=68, 78 and 80)

PERSPECTIVE
Kornyshev *et al.*
Physics of 'the most important molecule': unraveling hidden abilities encoded in the structure of DNA

1463-9076(2010)12:39;1-S

NC unit trapped by fullerenes: a density functional theory study on $Sc_3NC@C_{2n}$ ($2n$ = 68, 78 and 80)†

Peng Jin,[ab] Zhen Zhou,[c] Ce Hao,[a] Zhanxian Gao,[a] Kai Tan,[d] Xin Lu*[d] and Zhongfang Chen*[b]

Received 4th November 2009, Accepted 13th April 2010
DOI: 10.1039/b923106d

Endohedral metallofullerenes (EMFs) with a trapped cluster size larger than four are rather scarce. Inspired by a recent experimental observation, we explored the possibility of encapsulating an unusual Sc_3NC unit in three representative fullerene cages, namely, C_{68}, C_{78} and C_{80}, by means of density functional computations. The geometries, electronic and electrochemical redox properties of the corresponding EMFs, $Sc_3NC@C_{2n}$ ($2n$ = 68, 78 and 80), were investigated. These novel EMFs all have very favorable binding energies, implying a considerable possibility for experimental realization. The recently observed m/z = 1121 peak in the mass spectroscopy was characterized as $Sc_3NC@C_{80}$. Notably the lowest-energy isomer of $Sc_3NC@C_{78}$ has a non-IPR C_{78} outer cage, the possibility to accommodate five atoms inside a fullerene as small as C_{68} is also intriguing. Moreover, the intracluster and metal-cage covalent interactions were revealed by a quantum theory of atoms in molecules study. Infrared absorption spectra and ^{13}C nuclear magnetic resonance spectra were also computed to assist future experimental characterization.

1. Introduction

Endohedral metallofullerenes (EMFs) are novel materials enclosing metal atoms or metal-containing clusters in fullerene cages.[1] A unique feature of EMFs is the existence of substantial charge transfer from the encased species to the outer frameworks. The transferred electrons will not only change the electronic properties of fullerenes, but also, more significantly, can stabilize the otherwise unstable fullerene cages. Some such examples are $Sc_2@C_{66}$,[2] $Sc_3N@C_{68}$,[3] $Sc_2C_2@C_{68}$,[4] $Sc_3N@C_{70}$,[5] $La@C_{72}$,[6] $La_2@C_{72}$,[7] $Ce_2@C_{72}$,[8] $DySc_2N@C_{76}$,[9] $Dy_3N@C_{78}$(II),[10] $Gd_3N@C_{82}$,[11] $M_3N@C_{84}$ (M = Tb,[12] Tm and Gd[13]), in which carbon frameworks violate the well-known isolated pentagon rule (IPR)[14] themselves and thus have not been observed as empty-cage fullerenes in the experiments.

The EMF family was considerably enriched since the discovery of trimetallic nitride template (TNT) EMFs, as exemplified by $Sc_3N@C_{80}$ in 1999.[15] Since then, a large number of homogeneous metal nitride clusterfullerenes (NCFs) such as $Sc_3N@C_{68}$,[3] $Sc_3N@C_{70}$,[5] $Sc_3N@C_{78}$,[16] $Gd_3N@C_{2n}$ ($2n$ = 80–88),[17] $Dy_3N@C_{2n}$ ($2n$ = 78–88),[18] $Tm_3N@C_{2n}$ ($2n$ = 76–88)[19] or mixed metal NCFs such as $MSc_2N@C_{80}$ (M = Y, Ce, Gd, Tb, Er),[20–27] $DySc_2N@C_{76}$[9] and $Lu_2ScN@C_{68}$[28] have been synthesized, characterized or isolated. So far, all cages with even carbon atoms ranging from C_{68} to C_{98} (with the "missing" C_{72} and C_{74}) can form endohedral nitride cluster structures.[1f] The TNT EMFs have become the largest member of the endohedral fullerene family containing non-IPR cages.

In the meantime, metal-carbide EMFs were also studied extensively from the first scandium-carbide metallofullerene, $Sc_2C_2@C_{84}$.[29] During the recent years, several of this kind of compounds such as $Sc_2C_2@C_{68}$,[4] $Sc_3C_2@C_{80}$,[30] $Sc_4C_2@C_{80}$,[31] $Sc_2C_2@C_{82}$,[32] $Y_2C_2@C_{82}$[33] and $Ti_2C_2@C_{78}$[34] have been reported. Other intriguing EMFs include the first non-scandium mixed metal NCF, $Lu_xY_{3-x}N@C_{80}$ (I) (x = 1, 2),[35] triple-metal-mixed NCF $ScYErN@C_{80}$,[36] scandium oxide clusterfullerene $Sc_4(\mu_3\text{-}O)_2@C_{80}$,[37] and the first hydrocarbon-containing EMF $Sc_3CH@C_{80}$.[38] All these promise an exciting future for fullerene chemistry.

In a recent study, Dorn *et al.* detected a peak with a mass-to-charge ratio of 1121 in the mass spectrum.[39] Chemical intuition tells us that very likely it is $Sc_3NC@C_{80}$ containing a NC unit (electronic state $(Sc^{3+})_3(NC)^{3-}@C_{80}^{6-}$), which is isoelectronic to the stable monoanion of $Sc_3C_2@C_{80}$.[30] With an otherwise unstable Sc_3NC cluster trapped inside, this would be a totally new type of EMF. However, some basic questions regarding this novel EMF are still pending: What is the structure of the observed m/z = 1121 peak? Is it $Sc_3NC@C_{80}$ as we intuitively guess? If yes, what is the charge state of the trapped NC unit? Can other carbon cages with a size smaller than 80 (such as C_{68} and C_{78}) encapsulate the Sc_3NC cluster too? How about their intracluster bonding natures as well as cluster-cage ones? How about their electronic and redox properties? In this work, we performed detailed density functional theory (DFT) computations to address these issues.

[a] *State Key Laboratory of Fine Chemicals, Dalian University of Technology, Dalian, 116024, P. R. China*
[b] *Department of Chemistry, Institute for Functional Materials, University of Puerto Rico, San Juan, Puerto Rico 00931. E-mail: zhongfangchen@gmail.com*
[c] *Institute of New Energy Material Chemistry, Institute of Scientific Computing, Nankai University, Tianjin 300071, P. R. China*
[d] *State Key Laboratory of Physical Chemistry of Solid Surface & Center for Theoretical Chemistry, College of Chemistry and Chemical Engineering, Xiamen University, Xiamen 361005, P. R. China. E-mail: xinlu@xmu.edu.cn*

† Electronic supplementary information (ESI) available: Coordinates of the optimized endohedral complexes, detailed data for IR and NMR spectra and a full citation of ref. 41. See DOI: 10.1039/b923106d

2. Computational methods

Full geometry optimizations with symmetry constraints were carried out using the PBE functional[40] with a double numerical plus polarization (DNP) basis set without frozen core. Several different locations and orientations of the endohedral Sc_3NC clusters inside the fullerene cages were considered to survey the potential energy surface of the EMFs under investigation. Harmonic frequency analyses, at the same theoretical level, were performed to characterize the nature of the obtained stationary points. When a saddle point was found, the mode following from the first imaginary frequency was employed to locate the local minimum. All the reported structures in this work are true local minima. The computed vibrational spectra using such a scheme well reproduced the experimentally measured data of various EMFs, [1f,g] which validates the reliability of our computational methods. Electron affinities and ionization potentials were computed at the PBE/DNP theoretical level for the lowest-energy isomers.

To evaluate the feasibility for the experimental realization of $Sc_3NC@C_{2n}$ ($2n$ = 68, 78 and 80), we computed their binding energies (E_b). E_b is defined as the difference between the total energy of an endofullerene and the sum of the total energies of the separated ground-state C_{2n} cage and encapsulated cluster (*i.e.*, $E_b = [E_{tot}(C_{2n}) + E_{tot}(M)] - E_{tot}(M@C_{2n})$).

The geometries were further reoptimized at the B3LYP/6-31G* theoretical level for the ^{13}C NMR computations, by using the Gaussian 03 package.[41] A gauge-independent atomic orbital method[42] was employed to compute the NMR spectra, in which the chemical shifts were first evaluated relative to C_{60}, then were referenced to the tetramethylsilane (TMS) (δ (C_{60}) 143.15 ppm *vs.* TMS).[43]

To gain more insight into the nature of intracluster interactions as well as those between the inner clusters and the cages, we performed a quantum theory of atoms in molecules (QTAIM) study on the above B3LYP/6-31G* geometries and wavefunctions using AIM2000 software.[44]

To derive theoretically their electrochemical redox potentials, we computed the geometries and total energies of $[Sc_3NC@C_{2n}]^q$ (q = 0, ±1, ±2) in 1, 2-dichlorobenzene (ODCB) solvent (dielectric constant 10.12). To describe solvent effects, the conductor-like screening model (COSMO)[45] was employed. For a given redox reaction in solvent, reduced form (solvent) → oxidized form (solvent) + e, the computed redox potential E^0 is defined by the equation

$$E^0 = \Delta G - 4.98$$

in which ΔG is the free energy change of the reaction and is approximated by the total electronic energy change of the reaction, and −4.98 (unit: eV) is the free energy change associated with the reference ferrocene/ferrocenium (Fc/Fc^+) redox couple.[46] The first two reduction and the first two oxidation potentials of $Sc_3NC@C_{2n}$ in ODCB can thus be derived.

Dmol^3 code, if not mentioned otherwise, was employed for all DFT computations.[47] The 3D molecular orbitals were visualized with the aid of gOpenmol program.[48]

3. Results and discussion

3.1 Geometries and electronic structures

$Sc_3NC@C_{80}$. Up to now, most of the reported cluster-fullerenes are based on C_{80} fullerene. Due to the closed-shell electronic configuration as well as large highest occupied molecular orbital and lowest unoccupied molecular orbital gap (HOMO–LUMO) of its hexaanion,[49] the IPR C_{80} cage (I_h: 31924) has a remarkable stability and is thus employed here to encase the Sc_3NC cluster. Various possible isomers were explored by placing the Sc_3NC cluster at different locations and with different orientations within the cage (see ESI,† only coordinates of local minima are listed). An isomer with C_{2v} symmetry (Fig. 1a, Table 1) is energetically the most favorable and thus has the ground-state structure. The five atoms of the Sc_3NC cluster within the C_{80} cage form a perfect plane with the inner C atom locating at the center of the Sc_3 plane, which is in strong contrast to $Sc_3N@C_{80}$ in which N is situated at the Sc_3 plane center. Detailed analyses of its Kohn–Sham molecular orbitals reveal that a valence state of $(Sc^{3+})_3(NC)^{3-}@C_{80}^{6-}$ can be assigned to the $Sc_3NC@C_{80}$. One of the Sc^{3+} cations is close to one hexagon passing through the C_2 axis of the cage, while each of the other two cations resides near one 5–6 bond (bond shared by pentagon and hexagon). The nearest Sc–C distance (R_{Sc-C}), Sc–N distance (R_{Sc-N}) of the Sc_3NC moiety and the nearest Sc-cage separation are 2.08, 2.10 and 2.22 Å, respectively. Thus, the covalent interaction between the Sc^{3+} ions and the NC unit is stronger than that between the Sc^{3+} cations and the C_{80}^{6-} cage (see next section for detailed bonding analysis). The computed N–C bond length (R_{N-C}) of the trapped Sc_3NC unit is 1.27 Å, suggesting the formation of a N═C double bond with an electronic state of $(N{=}C)^{3-}$.

Theoretically there is another possible structure, $Sc_3C_2@C_{79}N$, corresponding to the mass experiment signal of 1121. However, among the several different isomers we searched, the lowest-energy configuration of $Sc_3C_2@C_{79}N$ is more than 50 kcal mol^{-1} higher in energy than the above C_{2v} $Sc_3NC@C_{80}$ (Fig. 2, ESI†).

$Sc_3NC@C_{78}$. C_{78} cage can encapsulate several four-atom clusters, such as Sc_3N[16] and Ti_2C_2.[34] The IPR C_{78} (D_{3h}: 24 109) isomer is not only the parent cage of $Sc_3N@C_{78}$, but also energetically the most stable isomer of C_{78} hexaanion.[10,16] However, when encapsulating larger clusters such as Y_3N and Lu_3N, the EMFs based on the non-IPR isomer (C_2: 22 010, two adjacent pentagon pairs (APPs)) are energetically the most favorable.[10] To search stable isomers of $Sc_3NC@C_{78}$, we considered several isomers using both of the two fullerene cages and followed the same computational procedure as that of $Sc_3NC@C_{80}$. After optimization, a C_2 symmetrical isomer with the C_2: 22 010 cage holds the lowest energy (Fig. 1b, Table 1). In comparison, the isomers based on the D_{3h}: 24 109 cage are all higher in energy (>6 kcal mol^{-1}) due to the unsuitable cavity. Note that many similarities are found between $Sc_3NC@C_{78}$ and $Sc_3NC@C_{80}$. First, the electron configuration of the former, namely, $(Sc^{3+})_3(NC)^{3-}@C_{78}^{6-}$, resembles that of the latter. Second, the inner C atom also locates at the planar Sc_3 cluster center with the whole Sc_3NC moiety exhibiting a T shape.

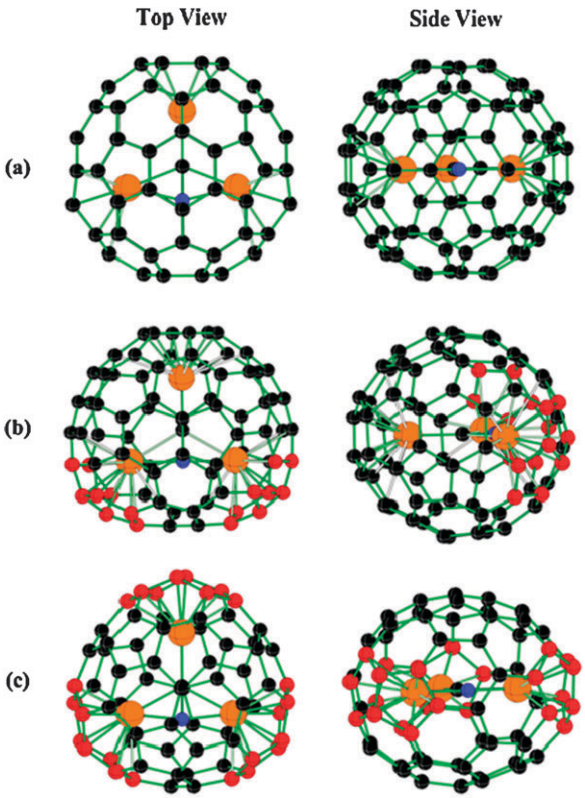

Fig. 1 (a) $Sc_3NC@C_{80}$ (C_{2v}), (b) $Sc_3NC@C_{78}$ (C_2) and (c) $Sc_3NC@C_{68}$ (C_2) isomers optimized at the PBE/DNP level of theory. The APPs are highlighted in red, Sc atoms in orange and N atoms in blue.

Table 1 Computed geometric parameters (Å) and HOMO–LUMO gap energies (eV) of the three lowest-energy $Sc_3NC@C_{2n}$ ($2n$ = 68, 78 and 80) isomers at the PBE/DNP level of theory[a]

Species	Symmetry	R_{Sc-C}	R_{Sc-N}	R_{N-C}	$R_{Sc-cage}$	Gap
$Sc_3NC@C_{80}$	C_{2v}	2.08	2.10	1.27	2.22	1.13 (2.29)
$Sc_3NC@C_{78}$	C_2	2.06	2.08	1.24	2.26	1.23 (2.23)
$Sc_3NC@C_{68}$	C_2	2.05	1.95	1.26	2.21	1.24 (2.12)

[a] B3LYP/6-31G* computed gap energies are listed in parentheses for reference.

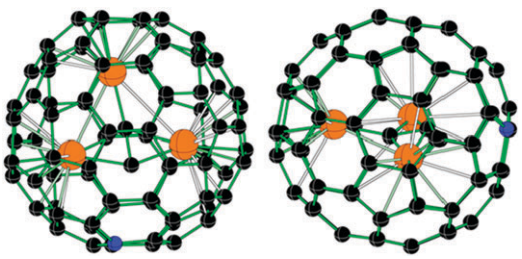

Fig. 2 The lowest-energy $Sc_3C_2@C_{79}N$ (C_1) isomer (two views) optimized at the PBE/DNP level of theory.

One Sc^{3+} cation locates near the top hexagon, while the other two are situated near the two APPs. Last, the R_{Sc-C} and R_{Sc-N} of the Sc_3NC moiety are 2.06 and 2.08 Å, respectively, also shorter than the $R_{Sc-cage}$ (2.26 Å). The R_{N-C} of the Sc_3NC unit is 1.24 Å. Thus, same valence state and double bond type as that of $Sc_3NC@C_{80}$ can be also assigned to this NC unit.

$Sc_3NC@C_{68}$. Thus far several metal-containing clusters, such as Sc_3N,[3] $DySc_2N$, $LuSc_2N$, Lu_2ScN,[28] have been trapped by non-IPR C_{68} (D_3: 6140) cage. For the inner moiety, an atom number larger than four has never been reported, which is apparently due to the limited cavity of the carbon cage. Since its hexaanion is energetically the most favorable[49] and has been proven to be the outer framework of the famous $Sc_3N@C_{68}$,[3] the non-IPR C_{68} (D_3: 6140) cage was chosen as the parent fullerene in this work. The C_{2v}: 6073 cage isomer was also considered to trap the Sc_3NC cluster, since its hexaanion is almost isoenergetic to that of the D_3: 6140.[49] However, the computed $Sc_3N@C_{68}$ isomers based on the C_{2v}: 6073 outer cage are all energetically unfavorable (by at least 68.9 kcal mol^{-1}, see ESI).†

The non-IPR C_{68} (D_3: 6140) cage has three isolated APPs. A C_2 isomer has the lowest relative energy and is the ground-state structure of $Sc_3NC@C_{68}$ (Fig. 1c). In the lowest-energy isomer, the Sc_3NC cluster inside the C_{68} cavity is perfectly planar with the inner C atom sitting at the center of the Sc_3 plane. Each Sc^{3+} cation coordinates to one APP. Clearly, this pattern is thermodynamically more stable, since the charges transferred from the metal cluster to the APPs formally convert the 8π antiaromatic pentalenes into 10π aromatic pentalene dianions.[50] The R_{Sc-C} and R_{Sc-N} of the Sc_3NC moiety are 2.05 and 1.95 Å, respectively, which are much shorter than the $R_{Sc-cage}$ (2.21 Å) (Table 1). The computed R_{N-C} of the trapped Sc_3NC unit is 1.26 Å. Thus, similar to the above two cases, a valence state of $(Sc^{3+})_3(NC)^{3-}@C_{68}^{6-}$ can be assigned to $Sc_3NC@C_{68}$.

Note that the isolated planar $(Sc_3NC)^{6+}$ cluster is not a local minimum according to our computation and thus can not exist by itself. Apparently, the interactions between the Sc_3NC moiety and the carbon frameworks simultaneously stabilize both the otherwise unstable five-atom cluster and the non-IPR cages. Moreover, for the above structures, the trapped Sc_3NC units are all planar. Initially we also considered structures trapping trifoliate Sc_3NC cluster, as in the case of $Sc_3C_2@C_{80}$.[30b] Interestingly, either the corresponding isomers are energetically unfavorable or the inner clusters turn to planar, after full optimizations. Moreover, all initial isomers with N atom instead of C atom residing at the center of the Sc_3 plane are all energetically unfavorable (see ESI).†

Further, the three ground-state structures all have very favorable binding energies (786.1 (717.7), 804.1 (742.2) and 817.2 (756.2) kcal mol^{-1} for $Sc_3NC@C_{68}$, $Sc_3NC@C_{78}$ and $Sc_3NC@C_{80}$, respectively) at the PBE/DNP (B3LYP/6-31G*) theoretical level. These predicted binding energies reveal that encapsulating Sc_3NC cluster into fullerene cages is highly exothermic, which in turn shows that both the carbon cage and the encapsulated moiety are significantly stabilized in the endohedral form, and suggest a remarkable possibility to experimentally realize these EMFs. However, note that the binding energies (or encapsulation energies) are only used to theoretically evaluate the stabilities of EMFs, while in the experiments EMFs are typically generated by the high-temperature arc discharge method in which the encapsulated cluster is encaged during the formation process, not through the encapsulation process.

In addition, all these three EMFs have sizable HOMO–LUMO gap energies (1.24 (2.12) eV for $Sc_3NC@C_{68}$, 1.23 (2.23) eV for $Sc_3NC@C_{78}$, and 1.13 (2.29) eV for $Sc_3NC@C_{80}$, respectively) at the PBE/DNP (B3LYP/6-31G*) level of theory (Table 1), implying their substantial kinetic stabilities. For comparison, the experimentally available $Sc_2C_2@C_{68}$ has a HOMO–LUMO energy gap of 0.68 eV at the PBE/DNP level of theory,[51] the experimentally well characterized $Sc_3N@C_{68}$, $Sc_3N@C_{78}$ and $Sc_3N@C_{80}$ species, which differ from the Sc_3NC doped fullerenes by only one endohedral C atom, have HOMO–LUMO gap energies of 2.11, 2.28 and 2.21 eV, respectively, at the B3LYP/6-31G* level of theory.

For $Sc_3NC@C_{68}$, its HOMO − 1 mainly locates on the Sc_3NC cluster, whereas the HOMO, LUMO and LUMO + 1 are mostly contributed by the C_{68} cage (Fig. 3). While for $Sc_3NC@C_{78}$ and $Sc_3NC@C_{80}$, all four orbitals of the former and the HOMO − 1, HOMO and LUMO + 1 of the latter can be mainly attributed to the outer carbon frameworks, whereas the LUMO of $Sc_3NC@C_{80}$ prefers to be localized around the Sc_3NC moiety.

We further computed their vertical electron affinity (VEA), vertical ionization potential (VIP) as well as adiabatic electron affinity (AEA) and adiabatic ionization potential (AIP) to assist future experimental assignments. The calculated EA (VEA 2.76 eV, AEA 2.81 eV for $Sc_3NC@C_{68}$, VEA 2.91 eV, AEA 2.94 eV for $Sc_3NC@C_{78}$, VEA 3.31 eV, AEA 3.36 eV for $Sc_3NC@C_{80}$) and the IP (VIP 6.68 eV, AIP 6.63 eV for $Sc_3NC@C_{68}$, VIP 6.96 eV, AIP 6.89 eV for $Sc_3NC@C_{78}$, VIP 7.12 eV, AIP 7.09 eV for $Sc_3NC@C_{80}$) suggest that these three endofullerenes all have good electron-accepting capacity and are also rather stable against oxidation.

3.2 Bonding natures

Up to now, only in few studies has QTAIM been employed to disclose the bonding features of EMFs.[52–54] In a very recent work, Popov and Dunsch performed a thorough QTAIM analysis for four typical classes of EMFs and suggested that all types of bonding have a substantial covalent character.[54]

Here, we first focus on the intracluster interactions of the Sc_3NC unit. For the three EMFs, no metal–metal bond critical point (BCP) is found. In $Sc_3NC@C_{68}$, BCPs are found between Sc1 atom and the inner C atom, between Sc2 or Sc3 and N atom, as well as between N and C atom, respectively (Fig. 4), leading to four bond paths in the Sc_3NC cluster in total. The small electron density ρ_{bcp} (0.09 and 0.12 a.u. for Sc1–C and Sc2/Sc3–N, respectively) and the negative Laplacian $\nabla^2\rho_{bcp}$ (−0.07 and −0.10 a.u. for Sc1–C and Sc2/Sc3–N, respectively) suggest weak covalent interactions between metal atoms and the carbon or nitrogen atom (Table 2). The covalent nature is further confirmed by their small positive normalized kinetic energy density G_{bcp}/ρ_{bcp}values (<1 a.u.), negative normalized energy density H_{bcp}/ρ_{bcp}values as well as the large ratio of absolute value of potential energy density to kinetic energy density $|V_{bcp}|/G_{bcp}$ (>2). Although a small positive $\nabla^2\rho_{bcp}$(0.10 a.u.) and relatively large G_{bcp}/ρ_{bcp} value (1.65 a.u.) are computed for the BCP between the N and C atoms, the large ρ_{bcp} value (0.39 a.u.), the negative H_{bcp}/ρ_{bcp} value (−1.586 a.u.) as well as the $|V_{bcp}|/G_{bcp}$ ratio (1.961) indicate strong covalent bonding of the N–C unit.

Similar covalent interactions are present for the metal clusters inside $Sc_3NC@C_{78}$ and $Sc_3NC@C_{80}$ as well (Table 2). In the latter, however, additional BCPs are also located between Sc2/Sc3 atoms and the carbon atom. Accordingly, six bond paths exist for the Sc_3NC moiety of $Sc_3NC@C_{80}$. Besides, Sc2/Sc3–C BCP in $Sc_3NC@C_{80}$ has a large bond ellipticity, ε (2.82).

From the above, we can conclude that the Sc_3NC cluster has a covalent bonding nature, which is independent of the outer cages.

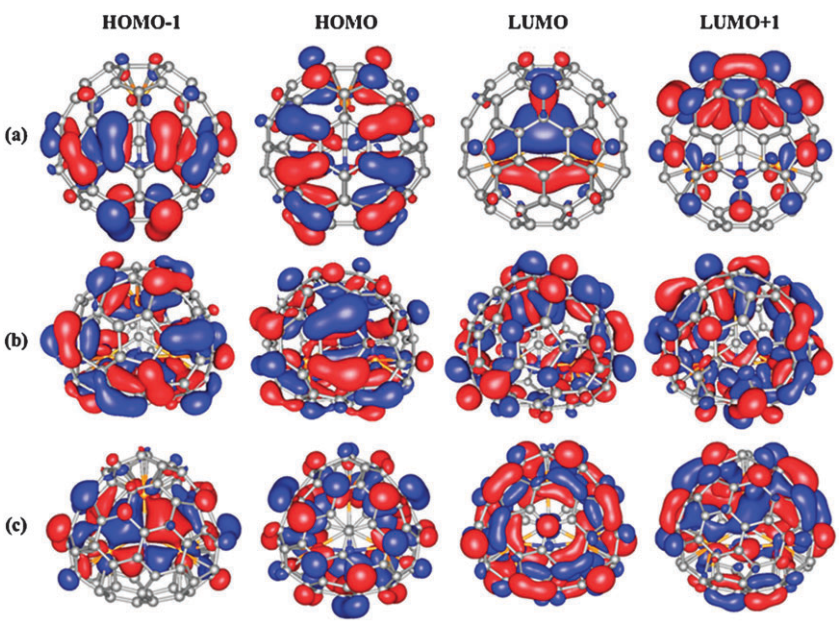

Fig. 3 Frontier orbitals of (a) $Sc_3NC@C_{80}$ (C_{2v}), (b) the $Sc_3NC@C_{78}$ (C_2) and (c) the $Sc_3NC@C_{68}$ (C_2) isomers.

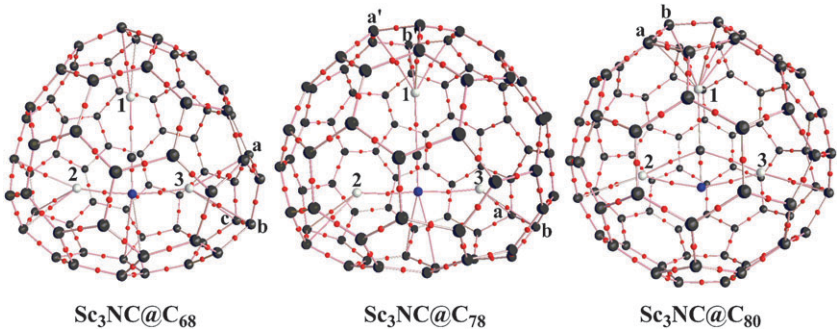

Fig. 4 Molecular graphs of the three EMFs (C black, Sc gray, N blue, BCP red). Ring and cage BCPs are omitted for clarity.

Table 2 QTAIM parameters for the trapped Sc_3NC clusters[a]

Species	A–B	R_{A-B}/Å	ρ_{bcp}	$\nabla^2\rho_{bcp}$	ε	G_{bcp}/ρ_{bcp}	H_{bcp}/ρ_{bcp}	$\lvert V_{bcp}\rvert/G_{bcp}$
$Sc_3NC@C_{68}$	Sc1–C	2.043	0.09	−0.07	0.40	0.586	−0.781	2.332
	Sc2/Sc3–N	1.943	0.12	−0.10	0.06	0.625	−0.833	2.333
	N–C	1.257	0.39	0.10	0.24	1.650	−1.586	1.961
$Sc_3NC@C_{78}$	Sc1–C	2.059	0.09	−0.07	0.40	0.554	−0.748	2.351
	Sc2/Sc3–N	2.072	0.09	−0.07	0.02	0.484	−0.678	2.402
	N–C	1.243	0.40	0.11	0.11	1.679	−1.611	1.959
$Sc_3NC@C_{80}$	Sc1–C	2.076	0.08	−0.07	0.40	0.566	−0.784	2.387
	Sc2/Sc3–C	2.186	0.07	−0.07	2.82	0.461	−0.711	2.543
	Sc2/Sc3–N	2.076	0.08	−0.08	0.21	0.544	−0.794	2.460
	N–C	1.267	0.39	0.12	0.21	1.614	−1.537	1.952

[a] Topological properties at the BCPs are in a.u.

More intriguing bonding features are found with regard to interactions between the inner clusters and the outer cages. The three Sc atoms in $Sc_3NC@C_{68}$ mainly bond to the 5–5 bonds of the cage. As discussed above, these are an ubiquitous feature for EMFs with non-IPR cages. Furthermore, an additional bond path is also found between Sc2 or Sc3 atom and one carbon atom of the related APP (Fig. 4, C_a). The N atom has two bond paths to the carbon atoms of a 6–6 bond at the bottom of the cage. For $Sc_3NC@C_{78}$, its Sc1 bonds to a hexagon with four bond paths, whereas each of Sc2 and Sc3 atoms bonds to a 5–6 edge; N atom di-coordinates to a near 6–6 bond, while in $Sc_3NC@C_{80}$, Sc1 has six bond paths to the carbon atoms of a cage hexagon, which can be grouped to two types (C_a and C_b) due to the C_{2v} symmetry. Sc2/Sc3 exhibits two equivalent bond paths to the carbon atoms of a 5–6 bond. Last, no BCP, thus no bond path was found between N atom and the carbon cage.

Although some differences exist among the molecular graphs of the three EMFs, QTAIM indicators suggest that they essentially have similar metal-cage interactions (Table 3). At all the Sc-cage BCPs, except their bond ellipticity ε, which can vary in a large range, they all exhibit small ρ_{bcp} values (<0.1 a.u.), negative $\nabla^2\rho_{bcp}$, small positive G_{bcp}/ρ_{bcp}(<1a.u.), negative H_{bcp}/ρ_{bcp} values as well as a large $|V_{bcp}|/G_{bcp}$ ratio. Thus, according to ref. 54, the bonding between metal clusters and the cages can be classified as covalent interactions with large polarity. The large ε values of certain BCPs (for instance, 9.49 for Sc1–C_a in $Sc_3NC@C_{80}$) indicate the Sc_3NC clusters within the fullerene cages are flexible and new BCPs are easy to be formed between them and the cages due to their tumble.

3.3 Electrochemical redox properties

The computed two oxidation potentials (+0.46 and +1.73 V for $Sc_3NC@C_{68}$, +0.76 and +1.62 V for $Sc_3NC@C_{78}$, +0.97 and +1.72 V for $Sc_3NC@C_{80}$) as well as the two reduction potentials (−1.19 and −1.91 V for $Sc_3NC@C_{68}$, −1.10 and −1.86 V for $Sc_3NC@C_{78}$, −0.80 and −1.94 V for $Sc_3NC@C_{80}$) in ODCB solvent are summarized in Table 4. The predicted electrochemical band gaps (1.65, 1.86 and 1.77 eV, respectively, for $Sc_3NC@C_{68}$, $Sc_3NC@C_{78}$ and $Sc_3NC@C_{80}$) are larger than many experimentally available EMFs such as $Sc_4C_2@C_{80}$ (1.56 eV, BLYP-DFT predicted value 1.65 eV).[31b] This indicates that these EMFs are very stable.

For $Sc_3NC@C_{68}$, its HOMO, LUMO and LUMO + 1 are mainly contributed by the C_{68} cage. As a result, its first oxidation state and the first two reduction states are predominantly related to the change of the carbon cage charge state. Thus for these reduction and oxidation states, the encapsulated cluster maintains its charge state as $(Sc^{3+})_3(NC)^{3-}$, and the NC moiety keeps its double bond (bond length around 1.26 Å). While a formal valence states $(Sc^{3+})_3(NC)^{-}@{C_{68}}^{6-}$ can be assigned for its second oxidation state, since the HOMO − 1 orbital mainly locates on the Sc_3NC cluster.

Similarly, the four frontier orbitals of $Sc_3NC@C_{78}$, are mainly localized on the carbon cages, thus the endocluster keeps its $(Sc^{3+})_3(NC)^{3-}$ charge state in $Sc_3NC@C_{78}$ with a negligible change of its NC bond length for the first and second reduction and oxidation states. Similar results are found in the two oxidation states of $Sc_3NC@C_{80}$.

Table 3 QTAIM parameters for the Sc_3NC-cage interactions[a]

Species	A–B	R_{A-B}/Å	ρ_{bcp}	$\nabla^2\rho_{bcp}$	ε	G_{bcp}/ρ_{bcp}	H_{bcp}/ρ_{bcp}	$\lvert V_{bcp}\rvert/G_{bcp}$
$Sc_3NC@C_{68}$	Sc1–C	2.220	0.07	−0.06	0.50	0.450	−0.664	2.476
	Sc2/Sc3–C_a	2.342	0.05	−0.05	7.79	0.435	−0.685	2.575
	Sc2/Sc3–C_b	2.209	0.07	−0.06	0.38	0.464	−0.679	2.462
	Sc2/Sc3–C_c	2.219	0.07	−0.06	0.77	0.450	−0.664	2.476
	N–C	2.624	0.02	−0.02	1.09	0.300	−0.550	2.833
$Sc_3NC@C_{78}$	Sc1–$C_{a'}$	2.296	0.06	−0.05	2.89	0.381	−0.590	2.546
	Sc1–$C_{b'}$	2.279	0.06	−0.05	1.71	0.397	−0.605	2.525
	Sc2/Sc3–C_a	2.258	0.06	−0.06	0.81	0.426	−0.676	2.587
	Sc2/Sc3–C_b	2.273	0.06	−0.05	0.50	0.434	−0.643	2.480
	N–C	2.600	0.02	−0.02	0.98	0.326	−0.576	2.767
$Sc_3NC@C_{80}$	Sc1–C_a	2.298	0.05	−0.05	9.49	0.455	−0.705	2.549
	Sc1–C_b	2.281	0.06	−0.05	2.26	0.396	−0.604	2.526
	Sc2/Sc3–C	2.213	0.07	−0.06	1.18	0.438	−0.650	2.492

[a] Topological properties at the BCPs are in a.u.

Table 4 Spin multiplicities (S), computed relative energies (E_{rel}, eV), and redox potentials (E^0, V) for $[Sc_3NC@C_{2n}]^q$ ($q = 0, \pm1, \pm2$) in ODCB solvent as well as the optimal N–C bond length (R_{N-C}, Å) and derived formal charge (Q_{N-C}) for the encapsulated NC moiety

	$Sc_3NC@C_{68}$					$Sc_3NC@C_{78}$					$Sc_3NC@C_{80}$				
q	+2	+1	0	−1	−2	+2	+1	0	−1	−2	+2	+1	0	−1	−2
S	1	2	1	2	1	1	2	1	2	1	1	2	1	2	1
E_{rel}	+12.15	+5.44	0.00	−3.79	−6.86	+12.34	+5.74	0.00	−3.88	−7.00	+12.65	+5.95	0.00	−4.18	−7.22
R_{N-C}	1.24	1.25	1.26	1.26	1.26	1.23	1.22	1.24	1.24	1.24	1.26	1.27	1.27	1.31	1.32
Q_{N-C}	−1	−3	−3	−3	−3	−3	−3	−3	−3	−3	−3	−3	−3	−4	−4
E^0	+1.73	+0.46		−1.19	−1.91	+1.62	+0.76		−1.10	−1.86	+1.72	+0.97		−0.80	−1.94

On the contrary, the 1-electron reduction of $Sc_3NC@C_{80}$ induces reduction of the encapsulated cluster, the inner cluster has a charge state of $(Sc^{3+})_3(NC)^{4-}$. Consequently, the NC bond is enlongated from 1.27 to 1.31 Å upon 1-electron reduction. More interesting is that the 2-electron reduction state has a N–C bond length of ~1.32 Å. Such a N–C bond length suggests a charge state of $(NC)^{4-}$. After checking the wavefunction of HOMO for the 2e reduction state, we found that this orbital is a hybrid of the cage and endocluster atomic orbitals.

3.4 Infrared and NMR spectra

The infrared (IR) absorption spectra of the $Sc_3NC@C_{68}$, $Sc_3NC@C_{78}$ and $Sc_3NC@C_{80}$ were computed at the PBE/DNP level (Fig. 5 and ESI).† Similar to that of $Sc_4C_2@C_{80}$,[31] each of their spectra can be roughly partitioned into three bands (from 1000 to 1700 cm^{-1}, from 300 to 900 cm^{-1} and blow 200 cm^{-1}). The first two bands are contributed by the vibrations of the carbon cages with the former having large absorption intensities. The third one consists of weak vibrations of the encased Sc^{3+} cations. The N–C stretching frequencies of the central NC units (1645, 1723 and 1582 cm^{-1} for $Sc_3NC@C_{68}$, $Sc_3NC@C_{78}$ and the $Sc_3NC@C_{80}$, respectively) all have very weak absorption intensities, which are also the highest vibrational wavenumbers of our computed spectra. Moreover, all of the strongest absorption peaks (1262, 1339 and 1342 cm^{-1} for $Sc_3NC@C_{68}$, $Sc_3NC@C_{78}$ and the $Sc_3NC@C_{80}$, respectively) correspond to the tangential vibrations of the carbon atoms along the cage surfaces. Several other relatively strong peaks (1360, 1374, 1428 cm^{-1} for $Sc_3NC@C_{68}$, 1340, 1360, 1378, 1392, 1398 cm^{-1} for $Sc_3NC@C_{78}$, 1307, 1309, 1366, 1381, 1423, 1522 cm^{-1} for $Sc_3NC@C_{80}$) may also help experimental characterization.

Theoretically simulated ^{13}C NMR spectra play an important role in the structural characterization of fullerenes

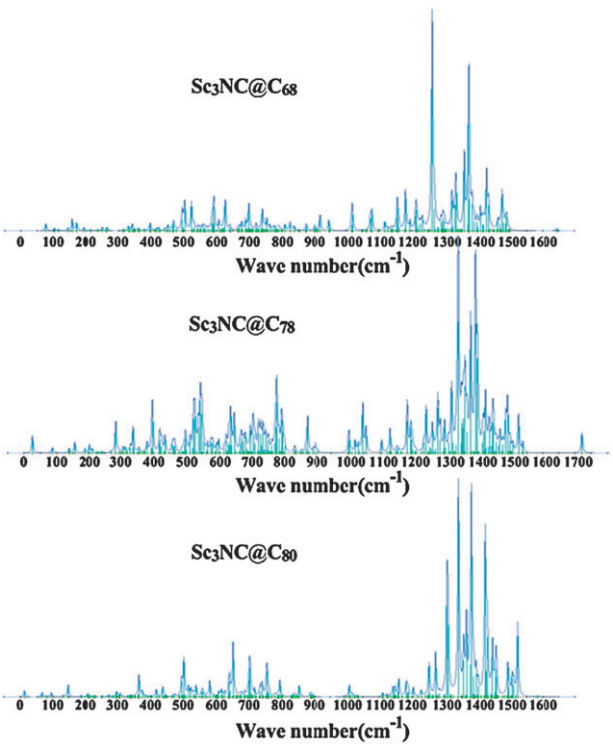

Fig. 5 The calculated IR vibrational spectra.

and their endohedral derivatives. According to their symmetries, the $Sc_3NC@C_{68}$ and $Sc_3NC@C_{78}$ exhibit 35 and 40 lines, respectively (Fig. 6). The bands ranging from 132 to 160 ppm are attributed to the carbon atoms of the outer cages. Far from the above bands, the chemical shifts of the central C atoms are 326.8 and 282.4 ppm for $Sc_3NC@C_{68}$ and $Sc_3NC@C_{78}$, respectively.

For $Sc_3NC@C_{80}$, the various isomers have rather small relative energy differences (<13 kcal mol^{-1}, ESI†). As a comparison, the rotation barriers of the Sc_3N unit inside the I_h C_{80} cage were computed to be *ca.* 2–3 kcal mol^{-1} using different theoretical methods.[55,56] Apparently, the inner cluster may tumble freely due to the large cavity and the smooth potential surface, similar to $La_2@C_{80}$,[57] $Sc_3N@C_{80}$,[15] $Sc_3C_2@C_{80}$[30] and $Sc_4C_2@C_{80}$.[31] Accordingly, to simulate its dynamic ^{13}C NMR spectrum, we computed the average chemical shifts for the triphenylenic sites (hexagon–hexagon–hexagon) and the corannulenic sites (hexagon–pentagon–hexagon) in $Sc_3NC@C_{80}$ separately. The calculated NMR chemical shifts are 137.3 ppm (low intensity) and 144.1 ppm (high intensity) for the triphenylenic sites and the corannulenic sites, respectively. Thus, ^{13}C NMR experiment on this molecule at room temperature would give 2 signals (137.3 and 144.1 ppm) for the C_{80} cage atoms. Yet, the NC carbon atom (chemical shift 306.6 ppm) may not be detectable due to spin-rotation interaction as well as its low atomic ration compared to those of the C_{80} cage.

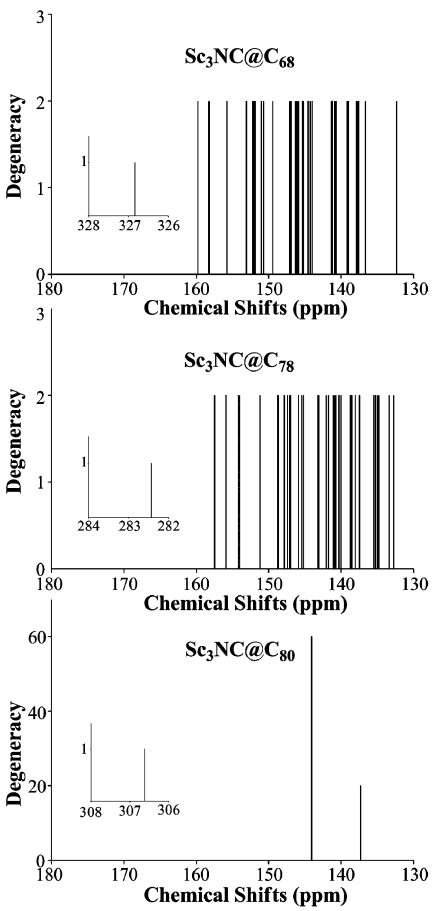

Fig. 6 The computed ^{13}C NMR spectra. The insets are chemical shifts of the NC carbon atoms.

4. Conclusions

In summary, as new members of the TNT EMF family, three typical fullerene cages trapping novel Sc_3NC units, namely, $Sc_3NC@C_{68}$, $Sc_3NC@C_{78}$ and $Sc_3NC@C_{80}$, were investigated by means of DFT computations. The Sc_3NC units all employ a planar structure within the cages. We can assign formal charge transfer of 6 *e* from the Sc_3NC moiety to the carbon frameworks, which stabilize both the otherwise unstable metal cluster and the fullerene cages simultaneously. The geometries with C centered at the Sc_3 planes are all energetically favored. All the lowest-energy EMFs hold very favorable binding energies, implying their promise for experimental realization. Our DFT computations characterized the recently observed m/z = 1121 peak in the mass spectroscopy to be $Sc_3NC@C_{80}$. Notably the lowest-energy isomer of $Sc_3NC@C_{78}$ has a non-IPR C_{78} outer cage, the possibility to accommodate five atoms inside a fullerene as small as C_{68} is also stimulating. Both intracluster and the metal-cage interactions were characterized as covalent by our detailed QTAIM analysis. The electronic, electrochemical redox properties as well as spectra were simulated to assist future experimental characterization. We believe that efforts from experimental peers will lead to the isolation of $Sc_3NC@C_{80}$ and its analogues, which will further enrich the famous TNT EMF family.

Acknowledgements

We thank Fengyu Li for carrying out several computations during the revision period. This work was supported in China by NSFC (20773018, 20873067, 20673088, 20425312, 20721001 and 20423002) and the 973 Program (2007CB815307), and in the USA by NSF Grant CHE-0716718, the Institute for Functional Nanomaterials (NSF Grant 0701525), and the US Environmental Protection Agency (EPA Grant No. RD-83385601). We thank Cong Wang for designing the cover picture.

References and notes

1 For recent reviews, see: (*a*) T. Akasaka and S. Nagase, *Endofullerenes: A New Family of Carbon Clusters*, Kluwer Academic Publishers, Dordrecht, The Netherlands, 2002; (*b*) H. Shinohara, *Rep. Prog. Phys.*, 2000, **63**, 843; (*c*) S. Guha and K. Nakamoto, *Coord. Chem. Rev.*, 2005, **249**, 1111; (*d*) L. Dunsch and S. F. Yang, *Electrochemical Society Interface*, 2006, **15**, 34; (*e*) N. Martin, *Chem. Commun.*, 2006, 2093; (*f*) L. Dunsch and S. F. Yang, *Small*, 2007, **3**, 1298; (*g*) L. Dunsch and S. F. Yang, *Phys. Chem. Chem. Phys.*, 2007, **9**, 3067; (*h*) M. Yamada, T. Akasaka and S. Nagase, *Acc. Chem. Res.*, 2010, **43**, 92; (*i*) M. N. Chaur, F. Melin, A. L. Ortiz and L. Echegoyen, *Angew. Chem., Int. Ed.*, 2009, **48**, 7514.
2 (*a*) C.-R. Wang, T. Kai, T. Tomiyama, T. Yoshida, Y. Kobayashi, E. Nishibori, M. Takata, M. Sakata and H. Shinohara, *Nature*, 2000, **408**, 426; (*b*) M. Takata, E. Nishibori, M. Sakata, C.-R. Wang and H. Shinohara, *Chem. Phys. Lett.*, 2003, **372**, 512.
3 (*a*) S. Stevenson, P. W. Fowler, T. Heine, J. C. Duchamp, G. Rice, T. Glass, K. Harich, E. Hajdu, R. Bible and H. C. Dorn, *Nature*, 2000, **408**, 427; (*b*) M. M. Olmstead, H. M. Lee, J. C. Duchamp, S. Stevenson, D. Marciu, H. C. Dorn and A. L. Balch, *Angew. Chem., Int. Ed.*, 2003, **42**, 900.
4 Z. Q. Shi, X. Wu, C.-R. Wang, X. Lu and H. Shinohara, *Angew. Chem., Int. Ed.*, 2006, **45**, 2107.
5 S. F. Yang, A. A. Popov and L. Dunsch, *Angew. Chem., Int. Ed.*, 2007, **46**, 1256.

6 T. Wakahara, H. Nikawa, T. Kikuchi, T. Nakahodo, G. M. A. Rahman, T. Tsuchiya, Y. Maeda, T. Akasaka, K. Yoza, E. Horn, K. Yamamoto, N. Mizorogi, Z. Slanina and S. Nagase, *J. Am. Chem. Soc.*, 2006, **128**, 14228.

7 (*a*) S. Stevenson, P. Burbank, K. Harich, Z. Sun, H. C. Dorn, P. H. M. van Loosdrecht, M. S. deVries, J. R. Salem, C.-H. Kiang, R. D. Johnson and D. S. Bethune, *J. Phys. Chem. A*, 1998, **102**, 2833; (*b*) H. Kato, A. Taninaka, T. Sugai and H. Shinohara, *J. Am. Chem. Soc.*, 2003, **125**, 7782; (*c*) X. Lu, H. Nikawa, T. Nakahodo, T. Tsuchiya, M. O. Ishitsuka, Y. Maeda, T. Akasaka, M. Toki, H. Sawa, Z. Slanina, N. Mizorogi and S. Nagase, *J. Am. Chem. Soc.*, 2008, **130**, 9129.

8 M. Yamada, T. Wakahara, T. Tsuchiya, Y. Maeda, T. Akasaka, N. Mizorogi and S. Nagase, *J. Phys. Chem. A*, 2008, **112**, 7627.

9 S. F. Yang, A. A. Popov and L. Dunsch, *J. Phys. Chem. B*, 2007, **111**, 13659.

10 A. A. Popov, M. Krause, S. F. Yang, J. Wong and L. Dunsch, *J. Phys. Chem. B*, 2007, **111**, 3363.

11 B. Q. Mercado, C. M. Beavers, M. M. Olmstead, M. N. Chaur, K. Walker, B. C. Holloway, L. Echegoyen and A. L. Balch, *J. Am. Chem. Soc.*, 2008, **130**, 7854.

12 C. M. Beavers, T. Zuo, J. C. Duchamp, H. C. Dorn, M. M. Olmstead and A. L. Balch, *J. Am. Chem. Soc.*, 2006, **128**, 11352.

13 T. Zuo, K. Walker, M. M. Olmstead, F. Melin, B. C. Holloway, L. Echegoyen, H. C. Dorn, M. N. Chaur, C. J. Chancellor, C. M. Beavers, A. L. Balch and A. J. Athans, *Chem. Commun.*, 2008, 1067.

14 (*a*) H. W. Kroto, *Nature*, 1987, **329**, 529; (*b*) T. G. Schmalz, W. A. Seitz, D. J. Klein and G. E. Hite, *J. Am. Chem. Soc.*, 1988, **110**, 1113; (*c*) P. W. Fowler and D. E. Manolopoulos, *An Atlas of Fullerenes*, Clarendon Press, Oxford, 1995.

15 S. Stevenson, G. Rice, T. Glass, K. Harich, F. Cromer, M. R. Jordan, J. Craft, E. Hadju, R. Bible, M. M. Olmstead, K. Maitra, A. J. Fisher, A. L. Balch and H. C. Dorn, *Nature*, 1999, **401**, 55.

16 M. M. Olmstead, A. de Bettencourt-Dias, J. C. Duchamp, S. Stevenson, D. Marciu, H. C. Dorn and A. L. Balch, *Angew. Chem., Int. Ed.*, 2001, **40**, 1223.

17 M. Krause and L. Dunsch, *Angew. Chem., Int. Ed.*, 2005, **44**, 1557.

18 S. F. Yang and L. Dunsch, *J. Phys. Chem. B*, 2005, **109**, 12320.

19 M. Krause, J. Wong and L. Dunsch, *Chem.–Eur. J.*, 2005, **11**, 706.

20 S. F. Yang, A. A. Popov, M. Kalbac and L. Dunsch, *Chem.–Eur. J.*, 2008, **14**, 2084.

21 S. F. Yang, M. Kalbac, A. A. Popov and L. Dunsch, *ChemPhysChem*, 2006, **7**, 1990.

22 (*a*) M. M. Olmstead, A. de Bettencourt-Dias, J. C. Duchamp, S. Stevenson, H. C. Dorn and A. L. Balch, *J. Am. Chem. Soc.*, 2000, **122**, 12220; (*b*) R. M. Macfarlane, D. S. Bethune, S. Stevenson and H. C. Dorn, *Chem. Phys. Lett.*, 2001, **343**, 229; (*c*) I. N. Ioffe, A. S. Ievlev, O. V. Boltalina, L. N. Sidorov, H. C. Dorn, S. Stevenson and G. Rice, *Int. J. Mass Spectrom.*, 2002, **213**, 183.

23 (*a*) E. B. Iezzi, J. C. Duchamp, K. R. Fletcher, T. E. Glass and H. C. Dorn, *Nano Lett.*, 2002, **2**, 1187; (*b*) S. Stevenson, H. M. Lee, M. M. Olmstead, C. Kozikowski, P. Stevenson and A. L. Balch, *Chem.–Eur. J.*, 2002, **8**, 4528.

24 X. L. Wang, T. M. Zuo, M. M. Olmstead, J. C. Duchamp, T. E. Glass, F. Cromer, A. L. Balch and H. C. Dorn, *J. Am. Chem. Soc.*, 2006, **128**, 8884.

25 N. Chen, L. Z. Fan, K. Tan, Y. Q. Wu, C. Y. Shu, X. Lu and C.-R. Wang, *J. Phys. Chem. C*, 2007, **111**, 11823.

26 N. Chen, E. Zhang, K. Tan, C.-R. Wang and X. Lu, *Org. Lett.*, 2007, **9**, 2011.

27 S. Stevenson, C. J. Chancellor, H. M. Lee, M. M. Olmstead and A. L. Balch, *Inorg. Chem.*, 2008, **47**, 1420.

28 S. F. Yang, A. A. Popov and L. Dunsch, *Chem. Commun.*, 2008, 2885.

29 C.-R. Wang, T. Kai, T. Tomiyama, T. Yoshida, Y. Kobayashi, E. Nishibori, M. Takata, M. Sakata and H. Shinohara, *Angew. Chem., Int. Ed.*, 2001, **40**, 397.

30 (*a*) Y. Iiduka, T. Wakahara, T. Nakahodo, T. Tsuchiya, A. Sakuraba, Y. Maeda, T. Akasaka, K. Yoza, E. Horn, T. Kato, M. T. H. Liu, N. Mizorogi, K. Kobayashi and S. Nagase, *J. Am. Chem. Soc.*, 2005, **127**, 12500; (*b*) K. Tan and X. Lu, *J. Phys. Chem. A*, 2006, **110**, 1171; (*c*) E. Nishibori, I. Terauchi, M. Sakata, M. Takata, Y. Ito, T. Sugai and H. Shinohara, *J. Phys. Chem. B*, 2006, **110**, 19215; (*d*) S. Taubert, M. Straka, T. O. Pennanen, D. Sundholm and J. Vaara, *Phys. Chem. Chem. Phys.*, 2008, **10**, 7158.

31 (*a*) K. Tan, X. Lu and C.-R. Wang, *J. Phys. Chem. B*, 2006, **110**, 11098; (*b*) T.-S. Wang, N. Chen, J.-F. Xiang, B. Li, J.-Y. Wu, W. Xu, L. Jiang, K. Tan, C.-Y. Shu, X. Lu and C.-R. Wang, *J. Am. Chem. Soc.*, 2009, **131**, 16646.

32 (*a*) Y. Iiduka, T. Wakahara, K. Nakajima, T. Nakahodo, T. Tsuchiya, Y. Maeda, T. Akasaka, K. Yoza, M. T. H. Liu, N. Mizorogi and S. Nagase, *Angew. Chem., Int. Ed.*, 2007, **46**, 5562; (*b*) R. Valencia, A. Rodríguez-Fortea and J. M. Poblet, *J. Phys. Chem. A*, 2008, **112**, 4550.

33 E. Nishibori, S. Narioka, M. Takata, M. Sakata, T. Inoue and H. Shinohara, *ChemPhysChem*, 2006, **7**, 345.

34 (*a*) K. Tan and X. Lu, *Chem. Commun.*, 2005, 4444; (*b*) T. Yumura, Y. Sato, K. Suenaga and S. Iijima, *J. Phys. Chem. B*, 2005, **109**, 20251.

35 S. F. Yang, A. A. Popov and L. Dunsch, *Angew. Chem., Int. Ed.*, 2008, **47**, 8196.

36 N. Chen, E.-Y. Zhang and C.-R. Wang, *J. Phys. Chem.B*, 2006, **110**, 13322.

37 S. Stevenson, M. A. Mackey, M. A. Stuart, J. P. Phillips, M. L. Easterling, C. J. Chancellor, M. M. Olmstead and A. L. Balch, *J. Am. Chem. Soc.*, 2008, **130**, 11844.

38 M. Krause, F. Ziegs, A. A. Popov and L. Dunsch, *ChemPhysChem*, 2007, **8**, 537.

39 H. C. Dorn, private communication.

40 J. P. Perdew, K. Burke and M. Ernzerhof, *Phys. Rev. Lett.*, 1996, **77**, 3865.

41 M. J. Frisch, *et al.*, *GAUSSIAN 03*, Gaussian Inc., Wallingford, CT, 2004. See Supplemetary Information for full reference.

42 K. Wolinski, J. F. Hilton and P. Pulay, *J. Am. Chem. Soc.*, 1990, **112**, 8251.

43 A. G. Avent, D. Dubois, A. Pénicaud and R. Taylor, *J. Chem. Soc., Perkin Trans. 2*, 1997, 1907.

44 (*a*) F. Biegler-König, AIM2000 version 1.0, University of Applied Sciences, Bielefeld, Germany, 2000; (*b*) R. F. W. Bader, *Atoms in Molecules a Quantum Theory*, Oxford University Press, Oxford, UK, 1990.

45 (*a*) A. Klamt and G. Schüürmann, *J. Chem. Soc., Perkin Trans. 2*, 1993, 799; (*b*) A. Klamt, V. Jonas, T. Bürger and J. Lohrenz, *J. Phys. Chem. A*, 1998, **102**, 5074.

46 M. F. Ryan, J. R. Eyler and D. E. Richardson, *J. Am. Chem. Soc.*, 1992, **114**, 8611.

47 (*a*) B. Delley, *J. Chem. Phys.*, 1990, **92**, 508; (*b*) B. Delley, *J. Chem. Phys.*, 2000, **113**, 7756. $DMol^3$ is available as part of Materials Studio and Cerius2 by Accelrys Inc.

48 (*a*) L. Laaksonen, *J. Mol. Graphics*, 1992, **10**, 33; (*b*) D. L. Bergman, L. Laaksonen and A. Laaksonen, *J. Mol. Graphics Modell.*, 1997, **15**, 301.

49 A. A. Popov and L. Dunsch, *J. Am. Chem. Soc.*, 2007, **129**, 11835.

50 T. K. Zywietz, H. Jiao, P. v. R. Schleyer and A. de Meijere, *J. Org. Chem.*, 1998, **63**, 3417.

51 Z. Q. Shi, X. Wu, C.-R. Wang, X. Lu and H. Shinohara, *Angew. Chem., Int. Ed.*, 2006, **45**, 2107.

52 K. Kobayashi and S. Nagase, *Chem. Phys. Lett.*, 1999, **302**, 312.

53 K. Kobayashi and S. Nagase, *Chem. Phys. Lett.*, 2002, **362**, 373.

54 A. A. Popov and L. Dunsch, *Chem.–Eur. J.*, 2009, **15**, 9707.

55 T. Heine, K. Vietze and G. Seifert, *Magn. Reson. Chem.*, 2004, **42**, S199.

56 J. M. Campanera, C. Bo, M. M. Olmstead, A. L. Balch and J. M. Poblet, *J. Phys. Chem. A*, 2002, **106**, 12356.

57 T. Akasaka, S. Nagase, K. Kobayashi, M. Wälchli, K. Yamamoto, H. Funasaka, M. Kako, T. Hoshino and T. Erata, *Angew. Chem., Int. Ed. Engl.*, 1997, **36**, 1643.